
Article:
Raza, A.R., Liu, W. orcid.org/0000-0003-2968-2888 and Shen, Q. (2019) Thinned coprime array for second-order difference co-array generation with reduced mutual coupling. IEEE Transactions on Signal Processing. ISSN 1053-587X

https://doi.org/10.1109/tsp.2019.2901380

Thinned Coprime Array for Second-Order Difference Co-Array Generation with Reduced Mutual Coupling

Ahsan Raza, Wei Liu, *Senior Member, IEEE,* and Qing Shen

***Abstract*—In this work, we present a new coprime array structure termed thinned coprime array (TCA), which exploits the redundancy in the structure of existing coprime array and achieves the same virtual aperture and degrees of freedom (DOFs) as the conventional coprime array with much fewer number of sensors. In comparison to other sparse arrays, thinned coprime arrays possess more unique lags (total number of difference co-arrays) than the nested arrays, while the number of consecutive lags (connected co-arrays) generated is close to 75 percent of the consecutive lags of the nested arrays with hole-free co-arrays. The resulting structure is much sparser and the number of sensor pairs with small separation is significantly reduced. Theoretical properties and proofs are provided and simulations are presented to demonstrate its robustness against heavy levels of mutual coupling using compressive sensing (CS) based direction of arrival (DOA) estimation as well as certain additional desirable characteristics.**

***Index Terms*—Mutual coupling, thinned coprime array, DOA estimation, degrees of freedom, difference co-array.**

I. INTRODUCTION

As well known already, higher number of degrees of freedom (DOFs) can be achieved by exploiting sparse arrays through the equivalent model of difference co-array [1–3]. These DOFs resulting from the difference in positions among different sensors represent the different lags at which the autocorrelation can be computed from the received data.

Two classic sparse array structures are the minimum redundancy array (MRA) [4, 5], and the minimum hole array (MHA) [6]. However, MRA and MHA do not possess closed-form expressions for the array geometry and the sensor positions are normally extracted from tabulated entries. To counter this deficiency, nested arrays are proposed [7], where exact expressions are available for sensor locations and number of DOFs achieved. Moreover, the hole-free property gives them an edge in their DOA estimation performance especially in the application of subspace based methods which rely on consecutive lags, but due to a densely packed subarray, they are prone to the effect of mutual coupling [8]. Another class of sparse arrays called coprime arrays can address this problem through a much sparser array design [9, 10]. Coprime and nested arrays offer certain advantages over MRAs and some other sparse array geometries. For example, depending on how they are processed, coprime arrays allow one to reduce peak sidelobe height by extending aperture, a property not found in most other common sparse arrays like MRAs or MHAs [11].

A coprime array consists of two uniform linear subarrays where one subarray has M sensors with Nd inter-element spacing, while the other subarray has N sensors with Md inter-element spacing, with M and N being coprime integers and d the unit spacing set to be $\frac{\lambda}{2}$ (λ corresponds to the wavelength of the impinging signal) [9]. This structure is referred to as the prototype coprime array with $M + N-1$ sensors and provides $2(M + N) - 1$ consecutive lags. To increase the number of consecutive lags, a modification was proposed in [10] by increasing the number of elements in one subarray from M sensors to $2M$ sensors. This structure of $2M + N - 1$ sensors termed as conventional coprime array resulting in $2MN + 2M - 1$ consecutive lags can be exploited using subspace based DOA estimation methods such as MUSIC [10, 12–15].

Two generalized coprime array configurations were recently proposed in [16] based on the prototype coprime array, where the first is based on compressing the inter-element spacing of the N-element subarray by a factor of M, resulting in a coprime array with compressed inter-element spacing (CACIS). The minimum inter-element spacing in CACIS remains unit spacing with considerable overlapping between self lags and cross lags. To counter this, a second type of array was proposed with a larger minimum inter-element spacing, larger aperture and higher number of unique lags, which is termed as coprime array with displaced subarrays (CADiS). It was shown that the CADiS structure performed much better than the CACIS structure for DOA estimation, and the compressive sensing (CS) based method can be employed without knowing the number of sources by forcing the sparsity across the potential incident angles [3, 16–18].

One factor not considered in many of the sparse array design schemes is the mutual coupling effect [19, 20]. Since most DOA estimation methods do not consider the effect, performance degradation will result when this effect is strong. Two approaches can be adopted to tackle this problem. The first one tends to incorporate the effect of mutual coupling and estimates the mutual coupling parameters along with the DOAs at the cost of extra computation and reduced DOFs [21–24]. The second route tries to reduce mutual coupling by designing sparser arrays. In this direction, super nested arrays were developed recently which hold all the advantages of nested

Ahsan Raza, Wei Liu and Qing Shen are with the Department of Electronic and Electrical Engineering, University of Sheffield, Sheffield, S1 3JD, UK (e-mail: smajafri1@sheffield.ac.uk, w.liu@sheffield.ac.uk, qingshen@outlook.com)

This work was partially supported by the National Natural Science Foundation of China (61628101 and 61801028).

arrays [25, 26]. It was shown that the third order super nested array was most robust to the effects of mutual coupling and performed better than the second order super nested array and other sparse arrays using MUSIC based DOA estimation methods. Most recently, an augmented nested array structure was proposed with enhanced DOF and reduced mutual coupling [27]. However, the mutual coupling of this structure could increase significantly with the increasing sensor number and even cause more mutual coupling than the super nested arrays. Concatenated nested array (CNA) has been recently proposed for active sensing with reduced mutual coupling [28]. A new nested multiple input multiple output (MIMO) array based on difference co-array of sum co-array has been proposed with careful design of interelement spacings of the transmitting and the receiving arrays [29]. It was shown that the array generates hole free difference co-arrays with enhanced DOFs for DOA estimation. A generalized nested array (GNA) with two flexible coprime factors for enlarging the interelement spacing of two concatenated uniform linear subarrays has been proposed which has the same DOFs as the nested array but with reduced mutual coupling [30].

As illustrated in [31], redundancy reduction in array structures require more snapshots to achieve a similar performance. Therefore, tradeoff has to be made between these two factors. In this paper, we focus on reducing the redundancy to improve the number of DOFs with reduced mutual coupling for a given number of sensors, and propose a new structure called thinned coprime array (TCA) by exploiting the redundancy in the difference co-array model of the conventional coprime array. As proved later in the paper, the lag contribution from some of the sensors in the $2M$-element subarray of the conventional coprime array is generated by the rest of the sensors in the array and these sensors can therefore be removed without affecting the properties of the parent array. The proposed TCA holds the same number of consecutive lags, unique lags and aperture as the conventional coprime array, but with $\lceil \frac{M}{2} \rceil$ fewer sensors, where $\lceil x \rceil$ returns the least integer greater than or equal to x. In comparison to other sparse arrays, for a fixed number of sensors, TCA achieves more unique lags than the total lags (hole free coarray) of a nested array, while generating about 75 percent consecutive lags of a nested array, producing a much larger and sparser aperture than the nested array. The work presented here is a further extension of our conference publication [32] and investigates the performance of the new structure from the perspective of mutual coupling. As an indication of the mutual coupling effect, the weight functions are also derived along with the proof and some new properties, which shows that the proposed TCA is robust against high level mutual coupling. The performance of TCA is thoroughly investigated in comparison to MRA, super nested arrays and CADiS for DOA estimation in the presence of mutual coupling using CS-based DOA estimation method and spatial smoothing (SS)-MUSIC.

This paper is organized as follows. The conventional coprime array is reviewed in Sec. II, followed by the proposed TCA in Sec. III. A comparison in terms of DOFs and mutual coupling between the TCA and other sparse arrays is provided in Sec. IV and Sec. V, respectively. Simulations results are provided in Sec. VI, with conclusions drawn in Sec. VII.

II. Conventional coprime array

Consider a conventional coprime array with $2M + N - 1$ sensors as shown in Fig. 1, where M and N are coprime integers. The array sensors are positioned at

$$\mathbb{P} = \{Mnd \mid 0 \leq n \leq N-1\} \cup \{Nmd \mid 0 \leq m \leq 2M-1\}. \tag{1}$$

The positions of the sensors are given by the set $\mathbf{p} = [p_0, ..., p_{2M+N-2}]^T$ where $p_i \in \mathbb{P}, i = 0, ..., 2M+N-2$. The zeroth sensor in both subarrays is co-located at the zeroth position with $p_0 = 0$.

Consider the scenario where Q uncorrelated signals are impinging on the array from angles $\Theta = [\theta_1, ..., \theta_Q]$ and their sampled baseband waveforms are expressed as $s_q(t), t = 1, ..., T$, for $q = 1, ..., Q$. Then, the data vector received by the coprime array is given by

$$\mathbf{x}(t) = \sum_{q=1}^{Q} \mathbf{a}(\theta_q) s_q(t) + \mathbf{n}(t) = \mathbf{A}\mathbf{s}(t) + \mathbf{n}(t), \tag{2}$$

where

$$\mathbf{a}(\theta_q) = [1, e^{-j\frac{2\pi p_2}{\lambda}\sin(\theta_q)}, ..., e^{-j\frac{2\pi p_{2M+N-1}}{\lambda}\sin(\theta_q)}]^T \tag{3}$$

is the steering vector of the array corresponding to θ_q, $\mathbf{A} = [\mathbf{a}(\theta_1), ..., \mathbf{a}(\theta_Q)]$ and $\mathbf{s}(t) = [s_1(t), ...s_Q(t)]^T$. The entries of the noise vector $\mathbf{n}(t)$ are white Gaussian with a covariance matrix $\sigma_n^2 \mathbf{I}_{2M+N-1}$, where σ_n^2 is the noise variance. The covariance matrix of data vector $\mathbf{x}(t)$ is given by

$$\begin{aligned} \mathbf{R_{xx}} &= E[\mathbf{x}(t)\mathbf{x}^H(t)] = \mathbf{A}\mathbf{R_{ss}}\mathbf{A}^H + \sigma_n^2 \mathbf{I}_{2M+N-1} \\ &= \sum_{q=1}^{Q} \sigma_q^2 \mathbf{a}(\theta_q)\mathbf{a}^H(\theta_q) + \sigma_n^2 \mathbf{I}_{2M+N-1}, \end{aligned} \tag{4}$$

where $\mathbf{R_{ss}} = E[\mathbf{s}(t)\mathbf{s}^H(t)] = \text{diag}([\sigma_1^2, ..., \sigma_Q^2])$ is the source covariance matrix, with σ_q^2 denoting the signal power of the qth source. In practice, the covariance matrix is estimated by

$$\hat{\mathbf{R}}_{\mathbf{xx}} = \frac{1}{T} \sum_{t=1}^{T} [\mathbf{x}(t)\mathbf{x}^H(t)]. \tag{5}$$

From the antennas located at the mth and nth positions in $\mathbf{p}$, the correlation $E[x_m(t)x_n^*(t)]$ results in the (m,n)th entry in $\mathbf{R_{xx}}$ with lag $p_m - p_n$. All the values of m and n, where $0 \leq m, n \leq 2M+N-2$, yield the lags or virtual sensors of the following difference co-array:

$$\mathbb{C}_{\mathbb{P}} = \{z \mid z = u - v, u \in \mathbb{P}, v \in \mathbb{P}\}. \tag{6}$$

III. THINNED COPRIME ARRAY

In this section we will show that all of the sensors in the $2M$-element subarray enclosed within the dashed rectangle in Fig. 1 are redundant and therefore can be removed without affecting the DOFs of the difference coarray, leading to the proposed thinned coprime array structure.

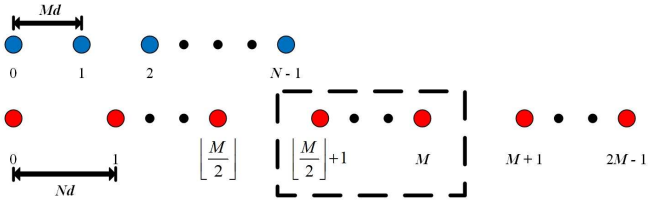

Fig. 1: Conventional coprime array.

A. The Proposed Thinned Coprime Array

Theorem 1. *The number of redundant sensors in a conventional coprime array with $M \geq 2$ for even M and $M \geq 5$ for odd M respectively are given by*

$$S_{red} = \left\lceil \frac{M}{2} \right\rceil, \tag{7}$$

where the starting index of these S_{red} contiguous redundant sensors in the $(2M-1)$-element subarray is given by $\lfloor \frac{M}{2} \rfloor + 1$.

Proof: The structure of the difference co-array can be divided into *self difference* i.e. diff($\mathbb{A}$, $\mathbb{A}$) and diff($\mathbb{B}$, $\mathbb{B}$) and *cross difference* i.e. diff($\mathbb{A}$, $\mathbb{B}$) and diff($\mathbb{B}$, $\mathbb{A}$), where $\mathbb{A}$ and $\mathbb{B}$ contain the sensor positions Mnd and Nmd respectively for the two subarrays with $0 \leq n \leq N-1$ and $0 \leq m \leq 2M-1$, while the diff operator stands for the difference between the positions of the sensors contained in the second set from the first set. In detail,

$$\begin{aligned}
&\text{diff}(\mathbb{A}, \mathbb{A}) = \{Mn_1 d - Mn_2 d \mid 0 \leq n_1, n_2 \leq N-1\},\\
&\text{diff}(\mathbb{B}, \mathbb{B}) = \{Nm_1 d - Nm_2 d \mid 0 \leq m_1, m_2 \leq 2M-1\},
\end{aligned}$$

$$\begin{aligned}
\text{diff}(\mathbb{A}, \mathbb{B}) = \{&(Mn - Nm)d\\
&\mid 0 \leq n \leq N-1, 0 \leq m \leq 2M-1\},
\end{aligned}$$

$$\begin{aligned}
\text{diff}(\mathbb{B}, \mathbb{A}) = \{&(Nm - Mn)d\\
&\mid 0 \leq n \leq N-1, 0 \leq m \leq 2M-1\},
\end{aligned}$$

Since all the self difference coarrays are included in the cross difference coarrays [33], we only need to check the redundancies in diff($\mathbb{A}$, $\mathbb{B}$). For the cross difference diff($\mathbb{A}$, $\mathbb{B}$), we use the index (n, m) to represent the lag entry $Mn - Nm$. It was shown in [33] that the entries in the cross correlation matrix associated with indices (n_1, m_1) and (n_2, m_2) in diff($\mathbb{A}$, $\mathbb{B}$) are complex conjugate of each other when the indices satisfy the following relationship

$$(n_1 + n_2)M = (m_1 + m_2)N \tag{8}$$

with the sufficient condition for (8) given by

$$(n_1 + n_2 = N) \cap (m_1 + m_2 = M). \tag{9}$$

This condition dictates that if we consider an index (n_1, m_1) with $0 \leq m_1 \leq \lfloor \frac{M}{2} \rfloor$ ($\lfloor x \rfloor$ returns the largest integer less than or equal to x) and $1 \leq n_1 \leq N-1$, then it will have a corresponding index (n_2, m_2) with $m_2 = M - m_1$ in the range $M - \lfloor \frac{M}{2} \rfloor \leq m_2 \leq M$ and $n_2 = N - n_1$ from $1 \leq n_2 \leq N-1$ with both indices satisfying (8). The corresponding entries of cross difference co-arrays with indices (n_1, m_1) and (n_2, m_2) satisfy the following relationship.

$$\begin{aligned}
\text{diff}(\mathbb{A}, \mathbb{B})^{n_1, m_1} &= -\text{diff}(\mathbb{B}, \mathbb{A})^{m_1, n_1} = -\text{diff}(\mathbb{A}, \mathbb{B})^{n_2, m_2}\\
&= -\text{diff}(\mathbb{A}, \mathbb{B})^{N-n_1, M-m_1}.
\end{aligned} \tag{10}$$

It thus follows that the lag entry corresponding to the index (n_2, m_2) of diff($\mathbb{A}$, $\mathbb{B}$) will be found in lag entry corresponding to index (m_1, n_1) of diff($\mathbb{B}$, $\mathbb{A}$), making the contribution of these lags from index (n_2, m_2) redundant.

Note that for index (n_1, m_1) with $m_1 = \lfloor \frac{M}{2} \rfloor = \frac{M}{2}$ when M is even, the corresponding redundant index (n_2, m_2) where $1 \leq n_1, n_2 \leq N-1$, will also have $m_2 = \frac{M}{2}$ with indices satisfying (8) and (10) respectively, and therefore $m = \frac{M}{2}$ for even M is not a redundant sensor. As a result, for arbitrary M and $1 \leq n \leq N-1$, the redundant sensor indices in the second sub-array are $\phi_r = \{\lfloor \frac{M}{2} \rfloor + 1, ..., M\}$.

Now we discuss the redundant sensors for $n = 0$ in the cross difference co-arrays and only the positive coarrays are analyzed due to its symmetric property. For any even $M \geq 2$, the lags from $(\frac{M}{2} + 1)N$ to MN associated with ϕ_r can be generated by taking the self difference of the $(M$ + 1)th sensor from the sensor indices 1 to $\frac{M}{2}$ in $\mathbb{B}$. Therefore, after removing the sensors in ϕ_r for even M, all the lags can be generated by the remaining sensors which proves the existence of $\lceil \frac{M}{2} \rceil$ redundant sensors shown by dashed rectangle in Fig. 1.

For the scenario where M is odd, we set $n = 0$ and to ensure the set ϕ_r still consists of redundant sensors, we assume that the lags from $\frac{M+1}{2}N$ to MN, related to the set ϕ_r can be generated by the remaining sensors. Considering the self difference of the $(M$ + 1)th sensor from sensor indices 1 to $\frac{M-1}{2}$, lags from $\frac{M+3}{2}N$ to MN can be generated. The $\frac{M+1}{2}N$ lag can be generated by taking difference of the $(M$ + 1)th sensor from the $(2M - \frac{M-3}{2})$th sensor where $(2M - \frac{M-3}{2})$ = $3\frac{M+1}{2}$th sensor. Then the following relationship should be satisfied to ensure the existence of the $3\frac{M+1}{2}$th sensor:

$$3\frac{(M+1)}{2} \leq 2M - 1, \tag{11}$$

which solves for $M \geq 5$. This result also proves the existence of the redundant sensor set ϕ_r with $\lceil \frac{M}{2} \rceil = \frac{M+1}{2}$ sensors shown by dashed rectangle in Fig. 1. ■

Instead of thinning redundant sensors from the conventional coprime array as mentioned in the proof, the TCA can be developed independently by a combination of three uniform linear subarrays in a straightforward way as follows.

Definition 1 (Thinned coprime array)**.** *Assume M and N are coprime integers with $M \geq 2$ for even M and $M \geq 5$ for odd M respectively, then the TCA is specified by the integer set* $\mathbb{X}$, defined by

$$\mathbb{X} = \mathbb{X}_1 \cup \mathbb{X}_2 \cup \mathbb{X}_3,$$

where

$$\begin{cases}
\mathbb{X}_1 = \{nMd \mid 0 \leq n \leq N-1\},\\
\mathbb{X}_2 = \{mNd \mid 1 \leq m \leq \lfloor \frac{M}{2} \rfloor\},\\
\mathbb{X}_3 = \{(m + M + 1)Nd \mid 0 \leq m \leq M-2\}.
\end{cases} \tag{12}$$

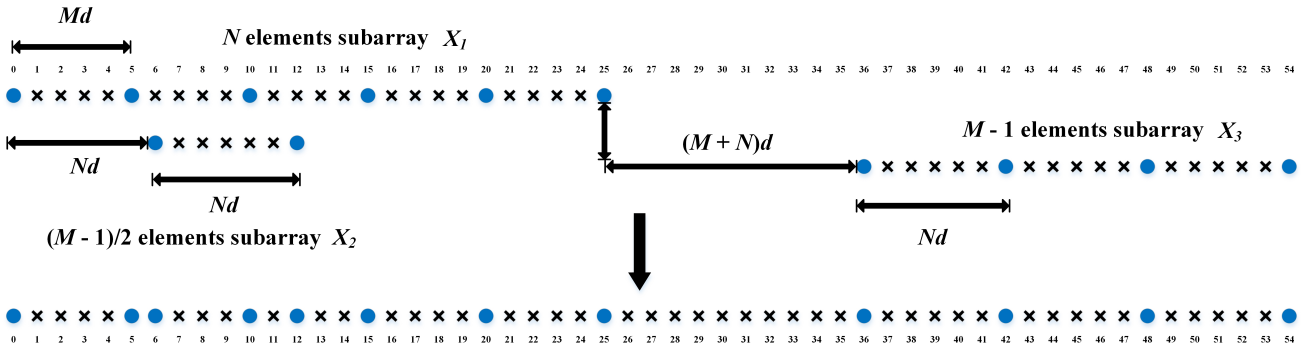

Fig. 2: Thinned coprime sensor array for M = 5, N = 6.

The sets $\mathbb{X}_1$, $\mathbb{X}_2$ and $\mathbb{X}_3$ represent the positions of sensors in the 1^{st}, 2^{nd} and 3^{rd} subarrays, respectively, which constitute the TCA. The total number of sensors is given by

$$S_{tcsa} = M + N + \lfloor \frac{M}{2} \rfloor - 1. \tag{13}$$

An example of the TCA with parameters M = 5 and N = 6 is shown in Fig. 2, where $\mathbb{X}_1 = \{0, 5, 10, 15, 20, 25\}d$, $\mathbb{X}_2 = \{6, 12\}d$ and $\mathbb{X}_3 = \{36, 42, 48, 54\}d$. The 3^{rd} subarray is displaced from the 1^{st} subarray by a spacing of $(M+N)d$ which in our case is $11d$ and is composed of $M - 1$ = 4 sensors separated by Nd = $6d$. By combining these three subarrays, the total number of sensors in the TCA is given by $M + N + \lfloor \frac{M}{2} \rfloor - 1 = 12$.

B. Optimal choice of M and N for TCA

For a TCA with $T = M + \lfloor \frac{M}{2} \rfloor - 1 + N$ sensors, the number of consecutive lags is $2MN + 2M - 1 = 2M(N + 1) - 1$. We can maximize the number of consecutive lags by applying the Arithmetic Mean-Geometric Mean (AM-GM) inequality to find the optimal choice of M and N [34].

Generally, the number of sensors can be expressed as $T = \frac{3}{2}M + N - 1 - \frac{\text{mod}\,(M,2)}{2}$. As a result, we have

$$\begin{aligned} 2M(N+1) - 1 &= \frac{4}{3}[\frac{3}{2}M(N+1)] - 1 \\ &\leq \frac{4}{3}\left(\frac{T + 1 + \frac{\text{mod}(M,2)}{2}}{2}\right)^2 - 1 \,, \end{aligned} \tag{14}$$

where the maximum value is obtained when $\frac{3}{2}M = N + 1$. The closer $\frac{3}{2}M$ and $N + 1$, the larger value can be achieved.

However, due to the existence of $\frac{\text{mod}(M,2)}{2}$, the maximum value achieved by odd M and even M are different, and it would be difficult to judge the optimal choice of M and N in general without the discussing the parity of M.

For odd M, the sub-optimal choice of M and N for a given T can be obtained by solving the following problem:

$$\begin{aligned} \min \quad & |\frac{3}{2}M - (N+1)| \,, \\ \text{subject to} \quad & \frac{3}{2}M + N = T + \frac{3}{2} \,, \\ & M \text{ is odd, } M \text{ and } N \text{ are coprime,} \end{aligned} \tag{15}$$

where $|\cdot|$ returns the absolute value of its argument, and the solutions are given by M_o and N_o.

Then for even M, we have

$$\begin{aligned} \min \quad & |\frac{3}{2}M - (N+1)| \,, \\ \text{subject to} \quad & \frac{3}{2}M + N = T + 1 \,, \\ & M \text{ is even, } M \text{ and } N \text{ are coprime,} \end{aligned} \tag{16}$$

and the solutions are M_e and N_e.

Finally, the maximum number of consecutive lags achieved is

$$\max\left(2M_oN_o + 2M_o - 1, 2M_eN_e + 2M_e - 1\right) \,, \tag{17}$$

and the corresponding M and N are the optimal choice for a fixed sensor number T.

IV. DOF COMPARISON OF SPARSE ARRAYS

In this section the number of DOFs provided by the proposed TCA, nested arrays, CADiS and its special cases for a fixed number of total sensors is compared, where DOFs presented in this paper represent two sided lags generated from the co-array structure of a sparse array.

Nested arrays for a given N_1 and N_2, where N_1 and N_2 represent the number of sensors in the two constituent subarrays, provide a hole free coarray of $2N_2(N_1+1)-1$ lags for a total of $N_1 + N_2$ sensors. The CADiS structure in [16] brings two changes to the existing prototype coprime array. In the first change, the first subarray of N sensors is compressed by a factor p where we assume $M = pM'$ for $2 \leq p \leq M$ with $1 \leq M' < M$ ($M' = 1$ is a special case for nested CADiS which will be discussed later). The resulting factors M' and N are still coprime. The elements of the first subarray then possess an interelement spacing of $M'd$, while the second subarray of M sensors retains the original interelement spacing of Nd. For the second change, it displaces the two subarrays by a factor Ld. The CADiS configuration for $M' > 1$ achieves a maximum number of unique lags equal to $2MN+2M-5$ when $L > N(M-2)$, while the maximum number of consecutive lags is achieved when $L = M' + N$ with $MN-(M'-1)(N-2)+1$ consecutive lags and $2MN+2M'-1$ unique lags [16]. The number of unique lags increases with increasing M' while the consecutive lags

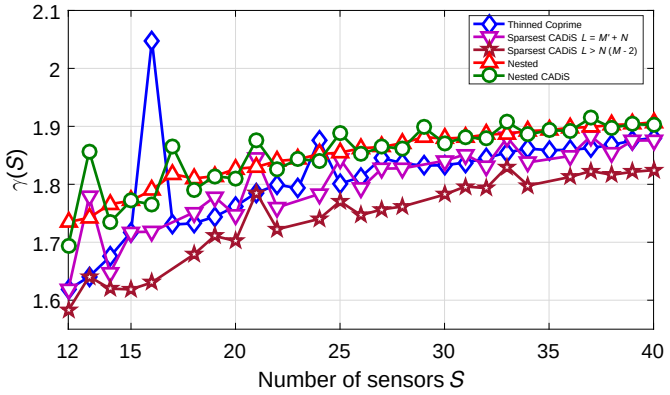

Fig. 3: Unique lags capacity comparison for sparse arrays.

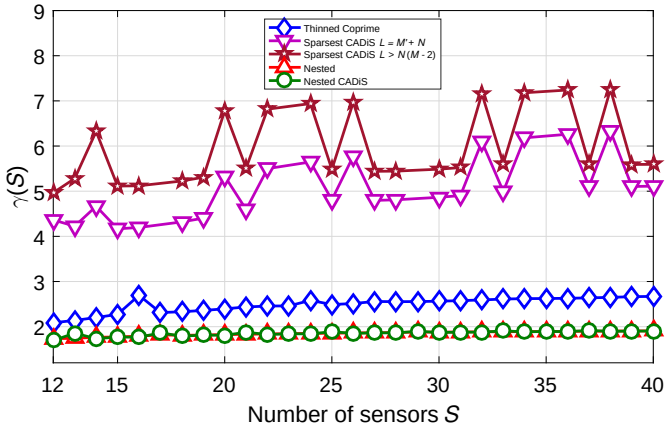

Fig. 4: Consecutive lags capacity comparison for sparse arrays.

decrease. Nested CADiS with $M'=1$ provides a hole-free co-array of $2MN+1$ lags. The proposed TCA retains all the properties of conventional coprime array, but with $\lceil \frac{M}{2} \rceil$ fewer sensors.

In the next step, we generate the number of DOFs including consecutive and unique lags for the sparse arrays under consideration. To further compare the sparsity of these array structures, we define the DOF capacity beyond the redundancy defined in [4] as

$$\gamma(S) = \frac{S^2}{DOFs} \tag{18}$$

where S represents the total number of sensors in an array and DOFs represents the number of degrees of freedom measured by the number of consecutive lags or unique lags. The smaller the value of $\gamma(S)$, the higher the DOF capacity with a specific number of sensors for that particular sparse array. Then the unique lags capacity for sparsest CADiS ($M' > 1$ with highest value of M' less than M and different cases of L), nested array, nested CADiS and TCA is plotted in Fig. 3, while the consecutive lags capacity is plotted in Fig. 4.

One potential problem in generating sparsest CADiS for any fixed number of sensors lies in the fact that sometimes the value of M available in combination with N to generate CADiS is a prime number itself (no factors for M other than 1), thus only offering the possibility of generating nested CADiS with $M' = 1$. For the analysis, all the available sparsest CADiS have been extracted, while nested arrays, nested CADiS and TCAs all can be generated for the considered range of sensors. The combinations of parameters have been chosen to produce the highest possible number of lags. It can be seen in Fig. 3 that the unique lags of TCA are comparable to the unique lags of the sparsest CADiS with $L = M' + N$, while the sparsest CADiS with $L > N(M-2)$ generates the highest number of unique lags. The number of unique lags of TCA are greater than the hole-free structure of nested array and nested CADiS as depicted in Fig. 3. It is further examined by taking the ratio of the number of unique lags produced by thinned coprime array to the lags produced by nested array for each sensor size scenario and then taking the mean which comes out as 1.0283. For the case of consecutive lags in Fig. 4, nested array and nested CADiS produce the highest number of consecutive lags. The number of consecutive lags of TCA are around 75 percent to those of nested array, which is calculated by taking the ratio of consecutive lags for TCA to the number of lags produced by nested array for each scenario of fixed number of sensors in the considered range of sensor array size and then calculating the mean of the ratio. The sparse versions of CADiS produce the lowest number of consecutive lags in comparison to the TCA, nested array and nested CADiS.

Another interesting thing is the non-availability of sparsest CADiS for 4 different cases of fixed number of sensors i.e. 17, 23, 29 and 35 due to reasons mentioned earlier. The points in the lags curve where there is a spike in the value of $\gamma(S)$ corresponds to a relatively lower increase in the DOFs for that specific number of sensors and is attributed to the value of M'. A larger M' available for one scenario will generate lower number of lags with resulting increase in the value of $\gamma(S)$. If a smaller M' is available for the next sensor array size, it will generate higher number of lags with a smaller $\gamma(S)$, giving the presence of a spike in $\gamma(S)$ for the former case. On the whole, sparse versions of CADiS cannot be generated for any arbitrary number of sensors and possess very low number of consecutive lags to be exploited by MUSIC based DOA estimation methods. Their application lies directly in the CS-based methods, where their unique lags can be utilized. TCAs can be generated for any arbitrary number of sensors and the number of unique lags are much higher than most of the sparse arrays and even the consecutive lags generated by TCA are on average around 75 percent of the hole-free coarray generated by nested arrays, which proves their application in both MUSIC and CS-based DOA estimation methods.

V. MUTUAL COUPLING PERSPECTIVE

A. Mutual Coupling Model

Equation (2) is free of mutual coupling. However, in practice, this is not avoidable and mutual coupling can be incorporated into the received signal model as follows.

$$\mathbf{x}(t) = \mathbf{CAs}(t) + \mathbf{n}(t) \tag{19}$$

where $\mathbf{C}$ is the mutual coupling matrix, which for uniform linear arrays can be modelled by a B-banded symmetric Toeplitz matrix [23, 25, 26], where B is chosen to be a suitable inter-sensor spacing beyond which the effect of mutual

coupling can be deemed negligible. The entries of the coupling matrix $\mathbf{C}$ in this case can be written as

$$\langle \mathbf{C} \rangle_{n_1,n_2} = \begin{cases} c_{|n_1-n_2|}, & \text{if } |n_1 - n_2| \leq B, \\ 0, & \text{otherwise} \end{cases} \tag{20}$$

where $n_1, n_2 \in \mathbf{p}$ and coupling coefficients $c_0, c_1, \ldots, c_B$ satisfy $1 = c_0 > |c_1| > |c_2| > \ldots |c_B|$. The magnitudes of coupling coefficients are inversely proportional to their sensor separations and one simple model is to assume

$$|\frac{c_k}{c_l}| = \frac{l}{k} \tag{21}$$

B. Mutual Coupling and Thinned Coprime Array

The effect of mutual coupling can be quantified with the help of weight function parameter defined in [25]. The weight function $w(m)$ of an array $\mathbf{p}$ refers to the number of sensor pairs corresponding to a particular value of coarray index m (which is an indication of the separation between the underlined sensor pair), and is given by

$$W(m) = \{(n_1, n_2) \in \mathbb{X}^2 \mid n_1 - n_2 = md\} \tag{22}$$

$$w(m) = \text{Card}(W(m)) \tag{23}$$

where $md \in \mathbb{C}_{\mathbb{P}}$ and $\text{Card}(A)$ returns the cardinality of the set A. The weight function values corresponding to small values of m would be of great interest as they contribute primarily towards mutual coupling in the array due to sensors separated by small multiples of interelement spacing. In this subsection, we present the weight functions of TCA along with the proof.

Theorem 2. *Let $\mathbb{X}$ be a thinned coprime array with $M \geq 2$ for even M and $M \geq 5$ for odd M respectively. Its weight functions w(m) for $m = 1, 2$ and 3 are given by*

$$\begin{cases} w(1) = \begin{cases} 2, & M = 2, \\ 1, & M \geq 4, \end{cases} \\ w(2) = \begin{cases} N-1, & \textit{if } M = 2, \\ \frac{3M-5}{2}, & \textit{if } N = 2, \\ 2, & \textit{if } M = 4, \\ 1, & \textit{otherwise,} \end{cases} \\ w(3) = \begin{cases} \frac{3M-4}{2}, & \textit{if } N = 3 \textit{ for any even } M, \\ \frac{3M-5}{2}, & \textit{if } N = 3 \textit{ for any odd } M, \\ 2, & \textit{if } (M = 2, N \geq 5) \textit{ or } M = 6, \\ 1, & \textit{otherwise,} \end{cases} \end{cases} \tag{24}$$

Proof: It is clear that the displacement between the third sub-array of the TCA and the others is at least more than $5d$ since M and N are coprime. Then we only consider the case when $\lfloor \frac{M}{2} \rfloor$ sensors of $\mathbb{X}_2$ interact with N sensors of $\mathbb{X}_1$. For any sensor of $\mathbb{X}_2$, there will be two sensors of $\mathbb{X}_1$ on either side of this sensor, resulting in 2 interactions per sensor with 2 lags less than the spacing Md for $\mathbb{X}_1$. For $\lfloor \frac{M}{2} \rfloor$ sensors of $\mathbb{X}_2$, this will result in a total of $2\lfloor \frac{M}{2} \rfloor$ lags contributing to the cross-difference set. Consider an arbitrary sensor of $\mathbb{X}_2$ located at iNd (d is ignored in the following analysis for simplification), where $1 \leq i \leq \lfloor \frac{M}{2} \rfloor$, and then the distance of this sensor relative to the nearest sensor of $\mathbb{X}_1$ lesser in value than iN is given by

$$S_i = \text{mod}(iN, M), 1 \leq i \leq \left\lfloor \frac{M}{2} \right\rfloor \tag{25}$$

where mod refers to the modulo operator and returns the remainder of $\frac{iN}{M}$. Likewise, the distance of any arbitrary sensor of $\mathbb{X}_2$ relative to the nearest sensor of $\mathbb{X}_1$ greater in value than iN is given by

$$\hat{S}_i = M - \text{mod}(iN, M), 1 \leq i \leq \left\lfloor \frac{M}{2} \right\rfloor \tag{26}$$

The lags generated from the interaction of any arbitrary sensor of $\mathbb{X}_2$ relative to two sensors of $\mathbb{X}_1$ surrounding it take the form $(S_i, \hat{S}_i)$. It can be shown that the lags in sets S_i and $\hat{S}_i$ repeat with a period of M. Substituting i with $i + M$ in (25) we have

$$\begin{aligned} S_{i+M} &= \text{mod}((i+M)N, M) \\ &= \text{mod}\ (iN, M) + \text{mod}(MN, M) = \text{mod}(iN, M) \end{aligned} \tag{27}$$

Similarly for $\hat{S}_i$,

$$\begin{aligned} \hat{S}_{i+M} &= M - \text{mod}((i+M)N, M) \\ &= M - \text{mod}(iN, M) - \text{mod}(MN, M) \\ &= M - \text{mod}(iN, M) \end{aligned} \tag{28}$$

As each lag in sets S_i and $\hat{S}_i$ repeats with a period M, this proves the unique nature of lags present within both sets S_i and $\hat{S}_i$ for $1 \leq i \leq \lfloor \frac{M}{2} \rfloor$. To analyze the scenario when the lag from one set also appears in the other set, we find the condition when $S_i = \hat{S}_j$ given by

$$\text{mod}\ (iN, M) = M - \text{mod}(jN, M), 1 \leq i, j \leq \left\lfloor \frac{M}{2} \right\rfloor \tag{29}$$

$$\text{mod}\ (iN, M) + \text{mod}(jN, M) = M \tag{30}$$

Applying modulo on both sides yields

$$\text{mod}(iN + jN, M) = \text{mod}(M, M) = 0 \tag{31}$$

Since M and N are coprime, the solution is given by

$$(i + j) = kM, k \in \mathbb{Z} \tag{32}$$

Since $1 \leq i, j \leq \lfloor \frac{M}{2} \rfloor$, the condition $(i + j) = kM$ cannot be satisfied for odd M. Then for even M, there exists $i = j = \frac{M}{2}$ that satisifes (32) with only one replicate lag at the $\frac{M}{2}$th sensor. As the lag values are of the form $(S_i, \hat{S}_i)$, this corresponds to values of these lags given as $(k, M - k)$ where $1 \leq k \leq M - 1$. For $k = \lfloor \frac{M}{2} \rfloor$, the lag pair will be equal to $(\lfloor \frac{M}{2} \rfloor, \lceil \frac{M}{2} \rceil)$. For even M, $i = j = \frac{M}{2}$ which implies that the repitition of lag for even M will occur at index $\frac{M}{2}$. To find the repeated value of lag pair at index $\frac{M}{2}$, we assume that this sensor in $\mathbb{X}_2$ is displaced from its corresponding two sensors of $\mathbb{X}_1$ by $\frac{M}{2}$. This corresponds to the position of the outer sensor of $\mathbb{X}_1$ relative to the $\frac{M}{2}$th sensor of $\mathbb{X}_2$ at $\frac{MN}{2} + \frac{M}{2} = \frac{M(N+1)}{2}$. Then we find the condition when $\frac{N+1}{2} \leq N - 1$ (the outermost index of $\mathbb{X}_1$), which solves for $N \geq 3$. This proves that the

repeated lag pair for even M occuring at index $\frac{M}{2}$ has a value equal to $\frac{M}{2}$. This value of repeated lag can also be alternatively checked by analyzing the case when for even M, lag pair $(\lfloor \frac{M}{2} \rfloor, \lceil \frac{M}{2} \rceil)$ reduces to $(\frac{M}{2}, \frac{M}{2})$. As a result $w(\frac{M}{2}) = 2$ for even M.

Now we discuss the different weight scenarios for even $M \geq 4$ and $N > 3$. Starting with $M = 4$, two sensors in $\mathbb{X}_2$ contribute four lags in total with values 1, 3 and two lags with values 2 proving $w(2) = 2$ and $w(1) = w(3) = 1$. For $M = 6$, three sensors in $\mathbb{X}_2$ contribute six lags in total with vaules 1, 5, 2, 4 and two lags with values 3 proving $w(3) = 2$ and $w(1) = w(2) = 1$. For $M > 6$ and $N > 3$, $w(1) = w(2) = w(3) = 1$ as the repeated lag for even M i.e. $\frac{M}{2} > 3$. For odd valued M with $N > 3$, the resulting lag pairs are all unique as shown above.

Then we consider some special cases. First when $N = 3$ and M is even, it is clear that $\frac{M}{2}-1$ pairs of sensors in $\mathbb{X}_2$ will be separated by a spacing of 3 in addition to $M-2$ pairs of sensors in $\mathbb{X}_3$. Adding the one unique lag equal to 3 from the interaction between the zeroth sensor of $\mathbb{X}_1$ and the first sensor of $\mathbb{X}_2$, then for any even M and $N = 3$, $w(3) = \frac{3M-4}{2}$. For the case of odd M and $N = 3$, the only difference is that $\frac{M-1}{2} - 1 = \frac{M-3}{2}$ pairs of sensors in $\mathbb{X}_2$ separated by 3, which will give an overall $w(3) = \frac{3M-5}{2}$. The case of odd M with $N = 2$ will also have $w(2) = \frac{3M-5}{2}$.

Finally we discuss the weights scenario when $M = 2$, resulting in one sensor contained in $\mathbb{X}_2$. This sensor through interaction with two sensors of $\mathbb{X}_1$ that are separated by a spacing of 2, contributes two lags in total with values 1 proving $w(1) = 2$. The value $w(2)$ depends on N as $N-1$ sensor pairs in the N-element subarray will be separated by inter-element spacing of 2 generating $w(2) = N-1$. For $w(3)$, we consider the case when $N \geq 5$, and then one sensor in $\mathbb{X}_2$ generating $w(1) = 2$ by falling in the middle of the two sensors of $\mathbb{X}_1$ will always be at a distance of 3 from the outer two sensors surrounding the two sensors of $\mathbb{X}_1$ on each side that generated $w(1)$, yielding $w(3) = 2$ for $M = 2$, $N \geq 5$.

As arrays with odd M provide $2\lfloor \frac{M}{2} \rfloor = 2\frac{M-1}{2} = M-1$ unique lags and the even valued M provide $M-2$ unique and two same valued lags with value $\frac{M}{2}$, it implies $w(1) = 1$ for $M \geq 4$. As $w(2) = 2$ only for $M = 4$, it proves $w(2) = 1$ otherwise. Likewise, $w(3) = 2$ for $M = 2$, $N \geq 5$ and $M = 6$ while $w(3) = 1$ otherwise, thus completing the proof. It is interesting to note that for any $M > 5$ and $N > 3$, thinned coprime arrays possess $w(1) = w(2) = w(3) = 1$. ∎

C. Array Profile Comparison and Mutual Coupling

In this subsection, a thorough comparison of several well-known sparse arrays is presented from the perspective of their sparsity, DOFs and potential to counter mutual coupling. The sparse arrays considered here include the proposed TCA, super nested arrays [25, 26], sparse CADiS [16] and MRA [4, 5][1]. First, a comparison of weight functions $w(m)$ for these sparse arrays is provided in Table I. It can be observed that although super nested arrays (both second order and higher orders) have smaller $w(1)$ and $w(3)$, their $w(2)$ is dependent on N_1 and thus increases with the array size. Sparse CADiS on the other hand has a zero-valued $w(1)$ and depending on the value of M, subsequently $M^{'}$, can have either $w(2)$ or $w(3)$ equal to $N-1$, which will also increase with increasing array size but overall maintain excellent sparsity. The proposed TCA has its weights $w(1)$, $w(2)$ and $w(3)$ independent of the array size and maintains $w(1)$ = $w(2)$ = $w(3)$ = 1 for odd $M \geq 5$ and even $M > 6$ with $N > 3$, which makes it a promising array structure to counter mutual coupling.

Sparse arrays also differentiate themselves from their characteristic DOFs (consecutive and unique). The application of a certain sparse array in subspace based methods like SS-MUSIC entirely depends on the consecutive lags, while CS-based DOA estimation utilizes all the unique lags generated and is applicable to all kinds of sparse arrays.

Keeping this view, a general character comparison of the considered sparse arrays is presented in Table II, where certain characteristics like availability for any array size, compatibility with CS, SS-MUSIC and relationship of critical weights functions with array size are provided. It is obvious that sparse CADiS finds its limitations in the use of SS-MUSIC as it generates very few consecutive DOFs. It is also not available for specific cases of array size as mentioned before, although it is excellent at tackling mutual coupling. Super nested arrays and MRA are good at SS-MUSIC and CS, but both have a problem of increasing critical weight $w(2)$ with array size, even for the sparsest of them, the third order super nested array as a function of N_1, which can create challenges to tackle heavy levels of mutual coupling. Suboptimal MRAs proposed by Ishiguro are also limited by the fact that arrays for more than 20 sensors are still not defined in [4, 5] due to the increase in complexity of the search mechanism and longer computation time to obtain MRA. The proposed TCA is available for any array size, applicable to both CS and SS-MUSIC as it provides a decent balance of consecutive and unique lags. This is further complemented by the sparse structure offered by TCA with consistent low weights irrespective of array size.

To have a further insight, we consider sparse arrays with a specific size of 12 sensors, comprised of two second order super nested arrays for the parameters $N_1 = N_2 = 6$ and $N_1 = 5$, $N_2 = 7$, one third order super nested array for $N_1 = 5$, and $N_2 = 7$, MRA as [0, 1, 6, 14, 22, 30, 38, 40, 42, 45, 47, 49]d [5], sparse versions of CADiS for $M = 6$, $N = 7$, $p = 2$ and 3, and thinned coprime array for $M = 5$ and $N = 6$. We have also incorporated MHA which has a characteristic weight function $w(m)$ equal to 0 or 1 for $m \neq 0$. The 12-sensor MHA considered here has sensor positions given by [0 2 6 24 29 40 43 55 68 75 76 85]d [35, 36]. For analysis, the mutual coupling model is based on (20) with $c_1 = 0.4e^{j\pi/3}$, $B = 10$ and $c_l = c_1 e^{-j(l-1)\pi/8}/l$ for $2 \leq l \leq B$. The analysis of these sparse arrays from different perspectives is provided in Fig. 5, where the weight functions $w(m)$ are provided in the second and sixth row of Fig. 5 and $|[\mathbf{C}]_{i,j}|^2$ is shown on log scale in the third and seventh row. The regions in dark indicate less energy

[1]Due to lack of explicit solutions for arrays with large number of sensors in [4], the MRAs with 12 sensors and 17 sensors employed in this paper are extracted from [5], which may be considered as a suboptimal solution instead of the strict MRA in [4].

Array	$SNA\ Q = 2$ $N_1 \geq 4$, $N_2 \geq 3$	$SNA\ Q \geq 3$, $(Odd\ N_1)$ $N_1 \geq 3 \times 2^Q - 1$, $N_2 \geq 3Q - 4$	$SNA\ Q \geq 3$, $(Even\ N_1)$ $N_1 \geq 2 \times 2^Q + 2$, $N_2 \geq 3Q - 4$	Sparse $CADiS$ $M = pM'$, $2 \leq p \leq M$, $1 \leq M' < M$	TCA $M \geq 2$ (even M), $M \geq 5$ (odd M)
$w(1)$	$\begin{cases} 2, & N_1 \textit{ is even,} \\ 1, & N_1 \textit{ is odd,} \end{cases}$	1	2	0	$\begin{cases} 2, & M = 2 \\ 1, & M \geq 4, \end{cases}$
$w(2)$	$\begin{cases} N_1 - 3, & N_1 \textit{ is even,} \\ N_1 - 1, & N_1 \textit{ is odd,} \end{cases}$	$2\lfloor \frac{N_1}{4} \rfloor + 1$	$\begin{cases} \frac{N_1}{2} + 1, & N_1 = 8k - 2, \\ \frac{N_1}{2} - 1, & N_1 = 8k + 2, \\ \frac{N_1}{2}, & \textit{otherwise}, k \in \mathbb{Z} \end{cases}$	$\begin{cases} N - 1, & \textit{if } M' = 2, \\ 0, & \textit{otherwise}, \end{cases}$	$\begin{cases} N - 1, & \textit{if } M = 2, \\ \frac{3M-5}{2}, & \textit{if } N = 2, \\ 2, & \textit{if } M = 4, \\ 1, & \textit{otherwise} \end{cases}$
$w(3)$	$\begin{cases} 3, & N_1 = 4, 6, \\ 4, & N_1 \textit{ is even}, N_1 \geq 8, \\ 1, & N_1 \textit{ is odd,} \end{cases}$	2	5	$\begin{cases} N - 1, & \textit{if } M' = 3, \\ 0, & \textit{otherwise}, \end{cases}$	$\begin{cases} \frac{3M-4}{2}, & \textit{if } N = 3 \textit{ for any even } M. \\ \frac{3M-5}{2}, & \textit{if } N = 3 \textit{ for any odd } M. \\ 2, & \textit{if } (M = 2, N \geq 5) \textit{ or } M = 6, \\ 1, & \textit{otherwise,} \end{cases}$

TABLE I: Weight function comparison for sparse arrays.

Array	SNA	Sparse $CADiS$	TCA	MRA
Availability for any array size	Yes	Not available for 17, 23, 29 and 35	Yes	Not available for more than 20 sensors
SS-MUSIC Compatibility	Yes	No	Yes	Yes
CS Compatibility	Yes	Yes	Yes	Yes
Relationship between critical mutual coupling coefficients and array size	$w(2)$ increases with array size	$w(2)$ or $w(3)$ may increase with array size but $w(1)$ = 0	$w(1) = w(2) = w(3)$ = 1 for odd $M \geq 5$ and even $M > 6$ with $N > 3$	$w(2)$ increases with array size for the suboptimal MRA's extracted from Ishiguro's work

TABLE II: Character comparison for sparse arrays.

for that particular entry and it is important to note that the off-diagonal entries of the matrix, i.e, the entries showing the interaction between different sensors, characterize the amount of mutual coupling for the sparse array. The darker these off-diagonal entries, the less the mutual coupling experienced by the particular sparse array. Looking at the coupling matrix structure, it is visible that the TCA and CADiS have less off-diagonal energy and more sparsity than the super nested arrays.

The array profile for these arrays is shown in Table III, highlighting different array characteristics like aperture, unique and consecutive lags, maximum number of detectable sources using SS-MUSIC and number of smaller weight functions like $w(1)$, $w(2)$ and $w(3)$. It is clear that MHA contains the highest number of unique lags equal to 133 with 95 consecutive lags. MRA generates the highest number of consecutive lags equal to 99 with a hole free co-array. Sparsest CADiS for $p = 2$ and thinned coprime array both attain unique lags equal to 89, followed by sparse CADiS for $p = 3$ with 87 lags and then the super nested arrays with 83 lags for a hole-free structure. Talking from the SS-MUSIC perspective which halves the available number of consecutive lags for application in DOA estimation, the sparsest structure of CADiS with $p = 2$ results in the lowest number of consecutive lags with only 16 number of sources able to be identified and resolved. As the segment of consecutive lags for CADiS is not centered around zero, for application of SS-MUSIC, the largest portion of consecutive lags is extracted from the available segments of consecutive lags in the coarray followed by the spatial smoothing technique to generate the covariance matrix based on the extracted co-array segment before applying MUSIC. In comparison to sparse CADiS, thinned coprime array, super nested arrays, MHA and MRA have a capacity to solve up to 34, 41, 47 and 49 sources respectively.

VI. Simulation Results for DOA Estimation

In this section, the DOA estimation performance of the considered sparse arrays is investigated under the effect of mutual coupling using both the CS-based method and the SS-MUSIC.

A. CS-based DOA Spectrum Under Heavy Mutual Coupling

To make use of all unique lags provided by each sparse array, the CS-based DOA estimation method is used as detailed in [32]. The parameters are 5 dB SNR, 1000 snapshots, 12 uncorrelated sources evenly spaced between $-60°$ and $60°$ with ϵ chosen empirically for a clear and fine DOA estimate. A scenario of heavy mutual coupling is assumed with $|c_1|=$ 0.4. A search grid of 3601 angles is formed in the full angle range with a step size of $0.05°$. The estimation results are shown in the fourth and eighth rows of Fig. 5.

It can be seen that the second order super nested array with $N_1 = N_2 = 6$ is missing 3 sources while the second and third order super nested arrays with $N_1 = 5$ and $N_2 = 7$ and MRA are all missing at least one source with the other two sources at extremely low powers and buried under the accompanying noise in the spectrum. Sparse CADiS with $p = 3$ has a noisy spectrum with the power of three sources being degraded while the sparsest CADiS with $p = 2$, TCA and MHA are able to resolve the 12 sources with a fine DOA spectrum in the presence of mutual coupling.

Array	$SNA^{(6,6,2)}$	$SNA^{(5,7,2)}$	$SNA^{(5,7,3)}$	$CADiS^{(6,7,2)}$	$CADiS^{(6,7,3)}$	$TCA^{(5,6)}$	MRA	MHA
Aperture	41	41	41	49	56	54	49	85
Uni. Lags	83	83	83	87	89	89	99	133
Con. Lags	83	83	83	38	33	69	99	95
Max. sources SS-MUSIC	41	41	41	18	16	34	49	47
$w(1)$	2	1	1	0	0	1	1	1
$w(2)$	3	4	3	6	0	1	4	1
$w(3)$	3	1	3	0	6	1	1	1

TABLE III: Sparse array characteristics for 12 sensors.

The three missing peaks for the second order super nested array with $N_1 = N_2 = 6$ are attributed to a higher $w(1)$ i.e. $w(1)$ = 2 compared to $w(1)$ = 1 for the other two super nested arrays and MRA which limits the use of this particular super nested array for lower values of $|c_1|$. The sparser structure of TCA, sparsest CADiS and MHA hold promising potential to counter mutual coupling using CS-based estimation method.

To have a better understanding of the benefits of the proposed TCA, another scenario is considered where a 17-sensor array receives 20 incoming signals with moderate SNR and heavy mutual coupling. The parameters set is 10 dB SNR, 1000 snapshots and a mutual coupling coefficient $|c_1|= 0.4$, while the remaining parameters are the same as above. It is obvious that for a 17-sensor array we are unable to generate sparse CADiS as described in Section IV. For other sparse arrays, we are able to generate second and third order super nested arrays for the choice of $N_1 = 9$ and $N_2 = 8$, MRA as [0, 1, 8, 18, 28, 38, 48, 58, 68, 78, 80, 82, 84, 87, 89, 91, 93]d [5], TCA for $M = 7$ and $N = 8$ and MHA with sensor positions given by [0, 5, 7, 17, 52, 56, 67, 80, 81, 100, 122, 138, 159, 165, 168, 191, 199]d [35].

MRA and super nested arrays have hole-free coarrays with 187 and 159 consecutive lags respectively, while TCA generates 125 consecutive lags and 167 unique lags. MHA generates 35 consecutive lags and 273 unique lags. The critical part of the analysis is the weight functions for these arrays. The second order super nested array has the highest $w(2)$ among all the arrays equal to 8 with $w(1) = w(3) = 1$, while $w(1) = 1$, $w(2) = 6$, $w(3) = 1$ for MRA, and $w(1) = 1$, $w(2) = 5$, $w(3) = 2$ for the third order super nested array. TCA and MHA both provide excellent set of weight functions with $w(1) = w(2) = w(3) = 1$. The estimation results are shown in Fig. 6, where it can be clearly seen that the super nested arrays and MRA are unable to distinguish all 20 sources and have a degraded spectrum with missing sources and lots of spurious peaks, while the TCA and MHA are able to detect all sources with a fine spectrum showcasing their potential to counter heavy mutual coupling when other sparse arrays are simply not available or not able to cope with the conditions.

To investigate the performance of these sparse arrays under the effect of mutual coupling, the root mean square error (RMSE) curves are calculated for varying intensity of mutual coupling coefficient $|c_1|$, varying number of snapshots T and across a range of different values of SNR.

B. RMSE Curves with Mutual Coupling Under Fixed and Dynamic Range SNR

Consider 10 narrowband sources with 12-sensor sparse arrays as presented in the simulation results for Fig. 5. First we present the CS-based results with varying mutual coupling intensity, where all the unique lags offered by the arrays are utilized. The parameters considered are 5 dB SNR, 1000 snapshots and $|c_1|$ varied from 0 to 0.7. The results are presented in Fig. 7, where each point is an average of 200 independent simulation runs. It can be observed that although MRA and super nested arrays possess lower error than CADiS and TCA, they are only capable of detecting all the sources in low to medium level of mutual coupling. For higher levels of mutual coupling, super nested arrays suffer heavily from missing sources, spurious peaks and degraded spectrum. MHA, sparsest CADiS and TCA are able to tolerate severe mutual coupling with minimum loss to the spectrum. TCA detects all sources till $|c_1|= 0.7$, while sparsest CADiS suffers from two source peaks degraded by the severe mutual coupling. MHA due to its very high unique lags and sparse structure has the lowest error of all. However, it has been observed that some extra peaks start appearing very close to an actual detected source, due to which peak detection gets complicated and estimation error for that source is influenced by the close proximity of the extra peak. This phenomenon happens from $|c_1|= 0.5$ onwards. As a result, the RMSE for MHA is shown till $|c_1|= 0.45$.

The RMSE results against the number of snapshots and SNR for $|c_1|= 0.3$ with remaining parameters same as before are shown in Figs. 8 and 9, respectively, where it can be seen that the MHA possesses the lowest RMSE due to high DOFs. MRA and super nested arrays with $w(1)$ = 1 are able to tolerate medium levels of mutual coupling and achieve better estimation performance compared to sparse CADiS and the TCA. Next, we present the SS-MUSIC based results. Fig. 10 shows the RMSE for varying mutual coupling intensity in the range of $|c_1|= 0$ to 0.2 with 10 dB SNR and 1000 snapshots. The shorter range of mutual coupling is assumed relative to the CS case keeping in mind the corresponding reduction in the DOFs when using SS-MUSIC. It can be observed that the TCA, despite having lower DOFs compared to MRA and super nested arrays, matches their performance as the mutual coupling level rises, due to the excellent sparsity offered by this structure. Sparse CADiS suffers from an increased error due to a dramatic reduction in the available number of DOFs for SS-MUSIC with only 18 and 16 for the sparse versions of CADiS considered. MHA with high consecutive lags maintains the lowest RMSE just like the CS case. For

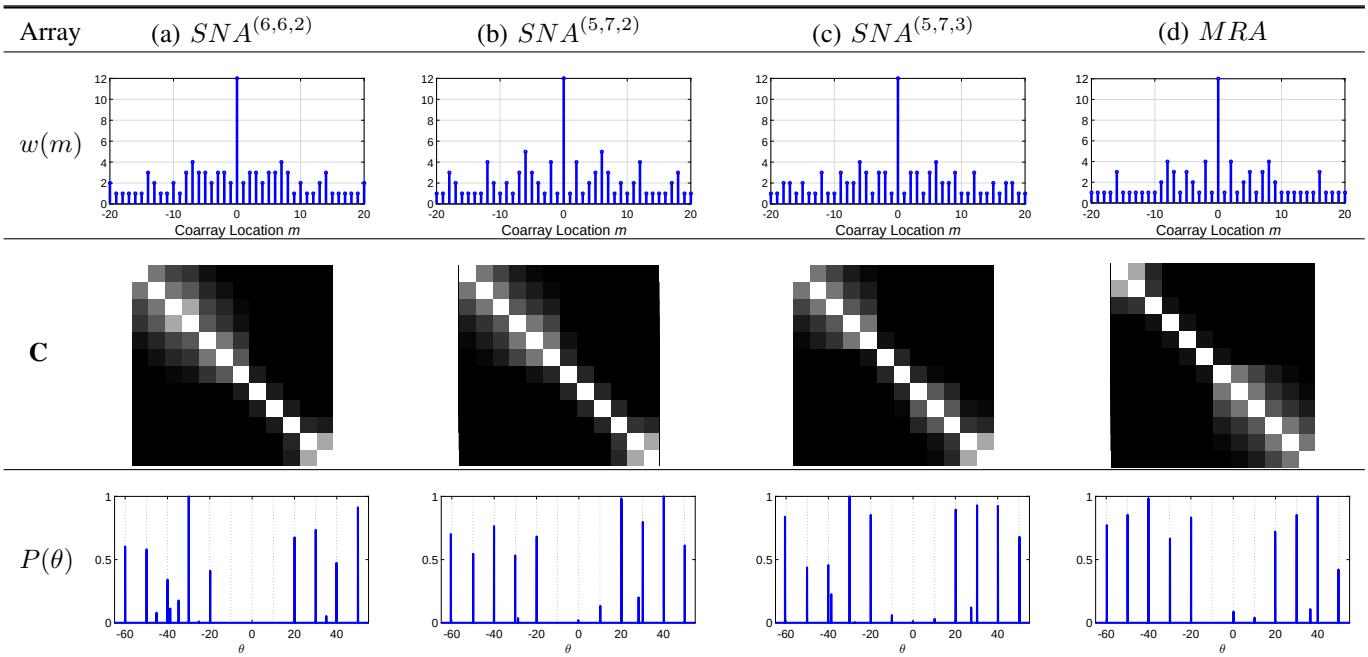

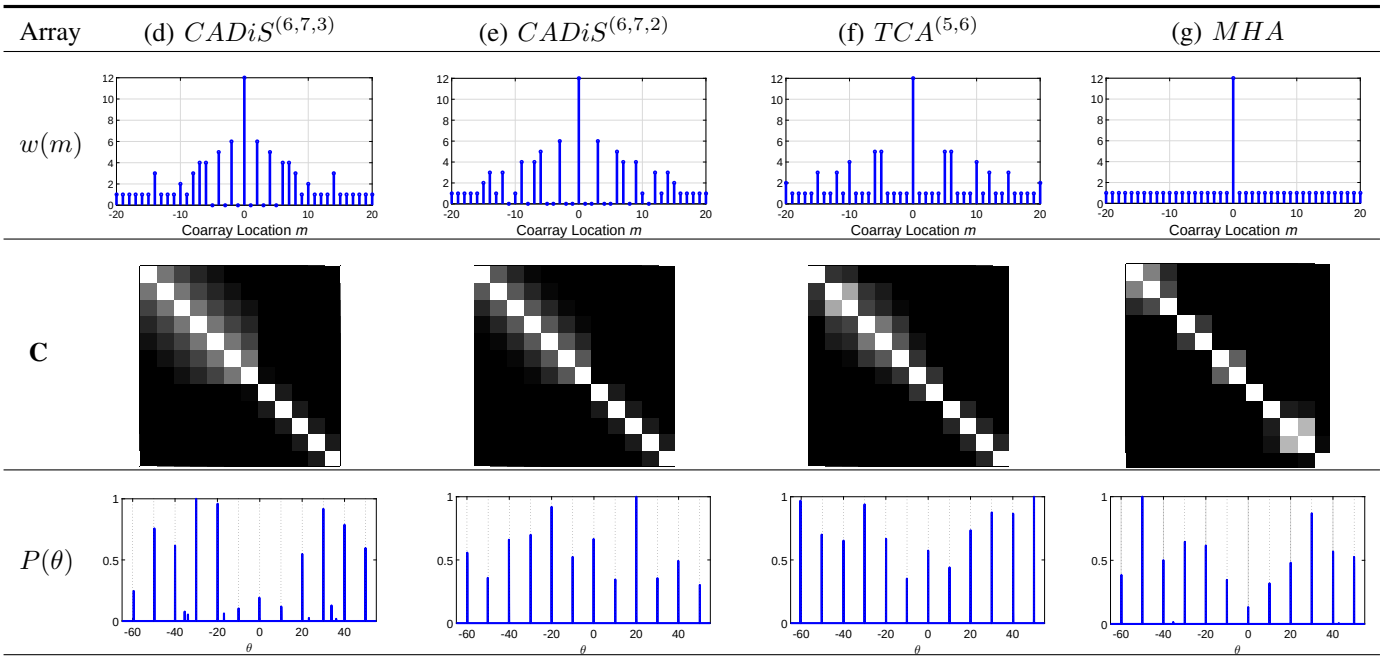

Fig. 5: Comparison among 12 sensors second order super nested array, third order super nested array, MRA, sparse CADiS , thinned coprime array and MHA in the presence of mutual coupling.

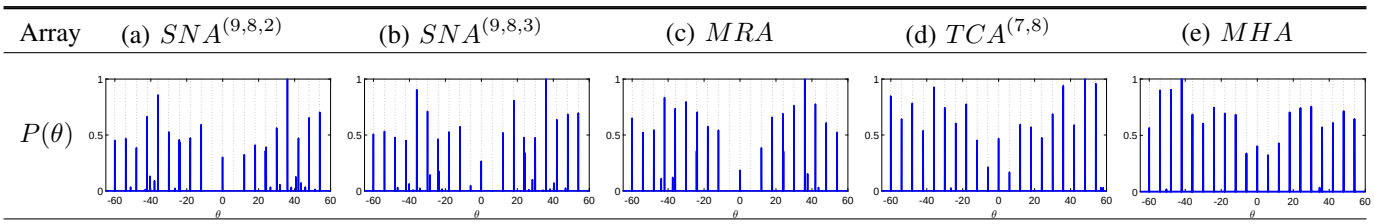

Fig. 6: Comparison among 17 sensors second order super nested array, third order super nested array, MRA, thinned coprime array and MHA in the presence of mutual coupling.

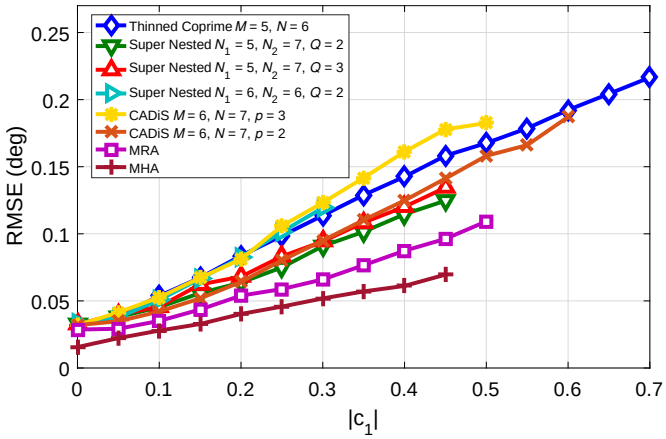

Fig. 7: RMSE versus mutual coupling coefficient $|c_1|$ for CS.

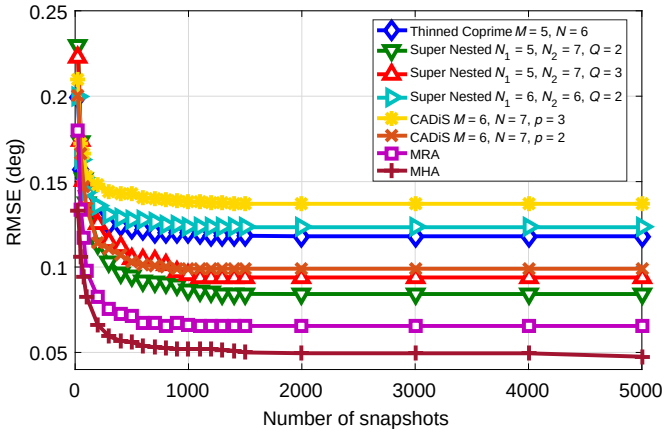

Fig. 8: RMSE versus number of snapshots for CS with $|c_1|$= 0.3.

RMSE curves against the number of snapshots and SNR, we consider $|c_1|$= 0.1 and the results are presented in Figs. 11 and 12, respectively. It is seen that TCA is able to perform better than super nested arrays and MRA as the SNR is increased while MHA has the lowest error of all the sparse arrays.

From a practical point of view, assuming equal SNR for all the sources is unrealistic. In real world, different sources impinging on an array are coming from different directions and from different distances with varying channel conditions, resulting in different SNR values for each of the sources. The way forward is to assume a 10 dB dynamic SNR range for the considered sources in the presence of mutual coupling, where the SNR of each source is uniformly distributed in the range [0, 10] dB. Then each source signal has a varying SNR in the range [0, 10] dB for each independent simulation run. The RMSE curves against varying mutual coupling for CS and SS-MUSIC in Figs. 7 and 10 are reproduced for dynamic SNR range in Figs. 13 and 14, respectively. Analyzing Fig. 13, due to the 10 dB dynamic range of SNR with more noisy conditions compared to fixed 5 dB in the previous case, the overall operational range of mutual coupling in the new results has reduced from $|c_1|$= 0.7 to 0.6. The results again show the robust nature of the proposed TCA. Although the array incurs increased error compared to super nested arrays, MRA and MHA, it is able to outperform all other sparse arrays in tackling heavy levels of mutual coupling. Furthermore, even the sparsest among sparse CADiS loses its application at $|c_1|$ = 0.5. MHA has the lowest error but with extra peaks just like the fixed SNR case has its RMSE limited to $|c_1|$= 0.45. In Fig. 14, it is clear that the error for sparse CADiS has increased a lot. It is directly in line with the use of dynamic range SNR as the low SNR for certain sources increases the overall error in the estimates and this effect is magnified by the lower number of DOFs available for sparse CADiS for SS-MUSIC. TCA is able to have a comparable performance to super nested arrays and MRA in this case.

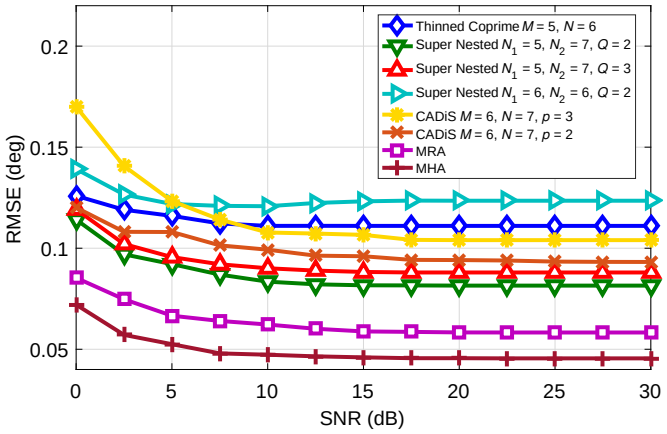

Fig. 9: RMSE versus SNR for CS with $|c_1|$= 0.3.

C. RMSE Curves with Mutual Coupling for Large Array Size

Now we consider a larger array size with 17 sensors utilized in Fig. 6. For this array size, all the sparse arrays are available except for the sparse CADiS. For CS based scenario, we

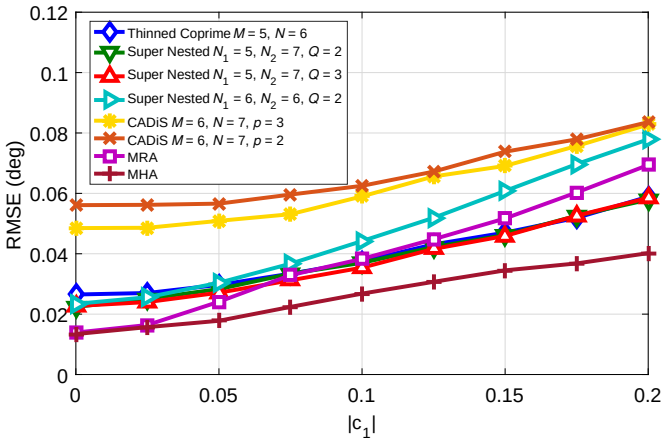

Fig. 10: RMSE versus mutual coupling coefficient $|c_1|$ for MUSIC.

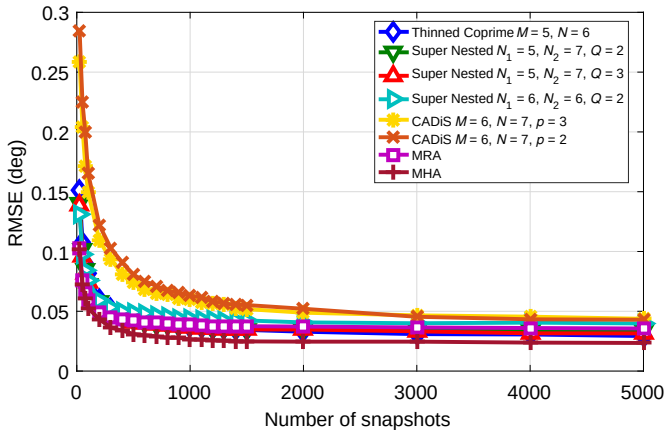

Fig. 11: RMSE versus number of snapshots for MUSIC with $|c_1|= 0.1$.

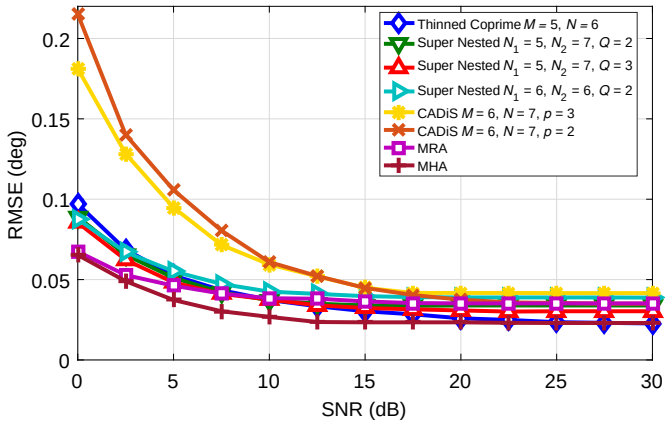

Fig. 12: RMSE versus SNR for MUSIC with $|c_1|= 0.1$.

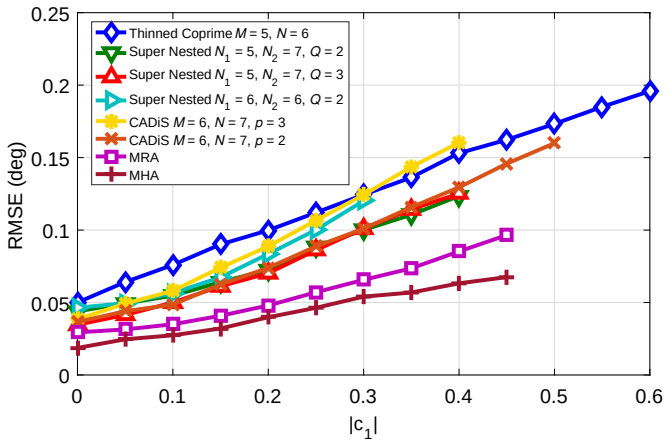

Fig. 13: RMSE versus mutual coupling coefficient $|c_1|$ with 10 dB dynamic range SNR for CS.

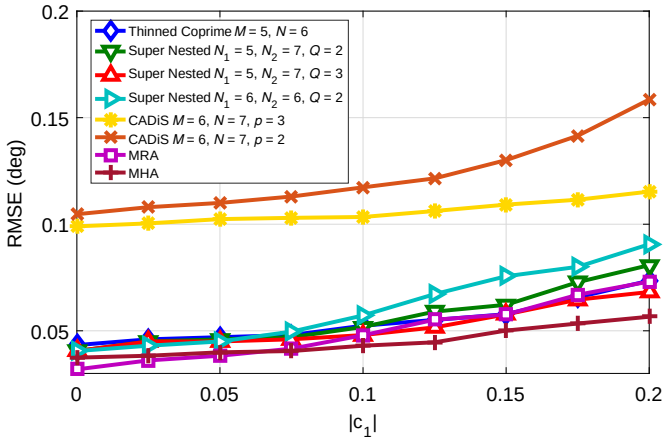

Fig. 14: RMSE versus mutual coupling coefficient $|c_1|$ with 10 dB dynamic range SNR for MUSIC.

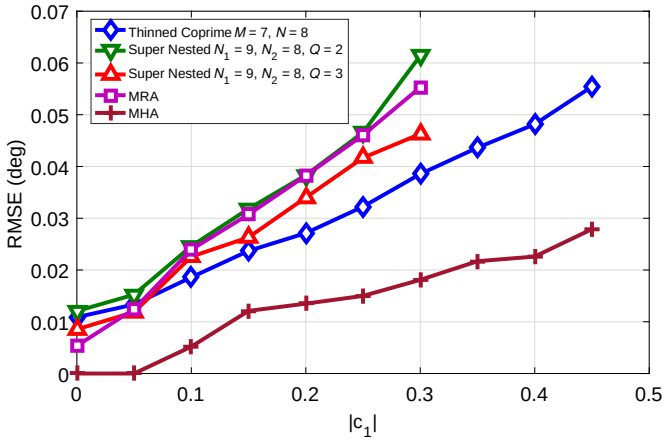

Fig. 15: RMSE versus mutual coupling coefficient $|c_1|$ with 17 sensors for CS.

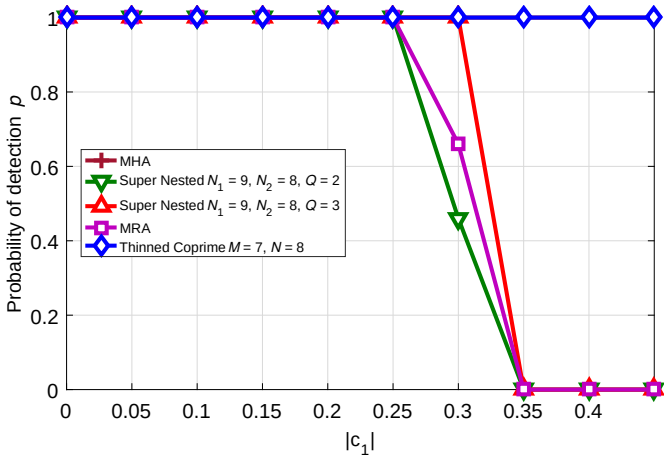

Fig. 16: Probability of detection versus mutual coupling coefficient $|c_1|$ with 17 sensors for CS.

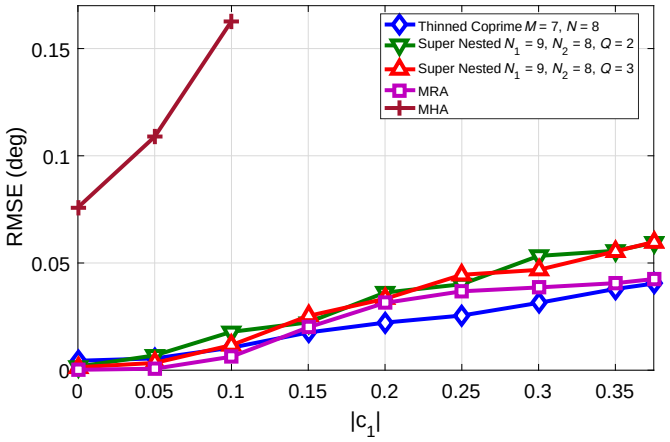

Fig. 17: RMSE versus mutual coupling coefficient $|c_1|$ with 17 sensors for MUSIC.

consider 20 sources, 10 dB SNR and 1000 snapshots with $|c_1|$ varying from 0 to 0.45. The result is shown in Fig. 15. It can be seen that MHA with very high number of unique lags equal to 273 has the lowest error among all the sparse arrays. TCA achieves a lower RMSE compared to MRA and super nested array with increasing levels of mutual coupling and is also able to tolerate high levels of mutual coupling. In comparison the operation range of super nested arrays and MRA is limited to $|c_1|$ = 0.3, where the third order super nested array has the lowest error compared to the second order super nested array and MRA due to its sparsity. This result shows that the error performance trend in the presence of mutual coupling varies significantly with increasing array size. As the DOFs rise in accordance with the array size, so do the critical weights for super nested arrays, suboptimal MRA's and even sparse CADiS. TCA due to its consistent critical weights of $w(1) = w(2) = w(3) = 1$ being independent of the array size is able to estimate sources with improved performance as the array size increases, while relatively higher errors are incurred by the super nested arrays and MRA due to a significant increase in $w(2)$.

A consequence of increased mutual coupling is the degradation of DOA spectrum. As the mutual coupling increases, source power reduces significantly till it appears as a missing source. For the result in Fig. 15, super nested arrays and MRA suffer from increased mutual coupling with their sources missing. The upper limit of their operation range is reduced to $|c_1|$ = 0.3, beyond which all independent simulation runs generate missing sources. A probability of detection curve is generated to show the probability p with which all sources are detected over a total number of independent simulation runs for a certain level of mutual coupling. It is worth noting that the RMSE results presented in Fig. 15 are based on the probability of detection shown in Fig. 16 against varying mutual coupling. It can be seen that the third order super nested array has 100 percent detection probability at $|c_1|$ = 0.3 compared to 66 and 46 percent for MRA and second order super nested array, respectively. Furthermore, TCA and MHA have 100 percent detection probability over the considered range of mutual coupling.

Then we investigate the performance of these arrays for SS-MUSIC. We consider 10 sources, 10 dB SNR, 1000 snapshots, $|c_1|$ varied from 0 to 0.375 with the result presented in Fig. 17. It can be seen again that the TCA despite having 63 DOFs to estimate 10 sources in comparison with 80 and 94 for super nested arrays and MRA respectively, is able to estimate the sources with the lowest error with increasing mutual coupling levels. MHA in this instance of 17 sensors is only able to generate 35 consecutive lags thereby suffering from a very high RMSE, which shows the limited applicability of MHA for SS-MUSIC for different array sizes. Moreover, MHAs are not defined for more than 26 sensors. In comparison, TCA with reasonable aperture, decent contribution of consecutive and unique lags and availability for any array size provides more application. This result achieved with SS-MUSIC complements the result achieved with CS and shows the real application of TCA with increasing array size and high mutual coupling.

Overall, the results have shown that the proposed TCA offers a set of excellent properties compared to other sparse arrays. Most important of all, the TCA is able to tolerate heavy levels of mutual coupling compared to super nested arrays, MRA and sparse CADiS. Due to a consistent sparse structure irrespective of array size, the TCA provides better performance than super nested arrays and MRA with increasing array size. Among all the extensions based on coprime array proposed till now, the proposed TCA is a better solution that can be effectively used with both CS and SS-MUSIC based DOA estimation in the presence of mutual coupling.

VII. CONCLUSION

In this paper, a new sparse array termed thinned coprime array has been proposed, which retains all the properties of the conventional coprime array, but with $\lceil \frac{M}{2} \rceil$ fewer sensors. For the same number of sensors, they possess greater number of unique lags than the hole-free structure of the nested array and nested CADiS, and comparable number of unique lags to the sparsest CADiS. The number of consecutive lags of the TCAs are around 75 percent to those of nested arrays which showcases their application in both subspace and CS-based DOA estimation methods. Moreover, they can be easily constructed for an arbitrary number of sensors. TCAs have a significantly sparser array structure with robustness against severe mutual coupling especially when using CS based DOA estimation. With increasing array size, TCAs also offer better performance in parameter estimation than super nested arrays and MRA for both CS and SS-MUSIC based methods in the presence of mutual coupling.

REFERENCES

[1] S. Pillai, *Array Signal Processing*. New York, NY, USA: Springer, 1989.

[2] H. L. Van Trees, *Optimum Array Processing, Part IV of Detection, Estimation, and Modulation Theory*. New York: Wiley, 2002.

[3] Q. Shen, W. Liu, W. Cui, and S. Wu, "Underdetermined DOA estimation under the compressive sensing frame-

work: A review," *IEEE Access*, vol. 4, pp. 8865–8878, 2016.

[4] A. Moffet, "Minimum-redundancy linear arrays," *IEEE Transactions on Antennas and Propagation*, vol. 16, no. 2, pp. 172–175, March 1968.

[5] M. Ishiguro, "Minimum redundancy linear arrays for a large number of antennas," *Radio Science*, vol. 15, no. 6, pp. 1163–1170, 1980.

[6] G. Bloom and W. Golomb, "Application of numbered undirected graphs," *Proc. IEEE*, vol. 65, no. 4, pp. 562–570, April 1977.

[7] P. Pal and P. P. Vaidyanathan, "Nested arrays: A novel approach to array processing with enhanced degrees of freedom," *IEEE Transactions on Signal Processing*, vol. 58, no. 8, pp. 4167–4181, Aug. 2010.

[8] I. Gupta and A. Ksienski, "Effect of mutual coupling on the performance of adaptive arrays," *IEEE Transactions on Antennas and Propagation*, vol. AP-31, no. 5, pp. 785–791, Sep 1983.

[9] P. P. Vaidyanathan and P. Pal, "Sparse sensing with co-prime samplers and arrays," *IEEE Transactions on Signal Processing*, vol. 59, no. 2, pp. 573–586, Feb. 2011.

[10] P. Pal and P. P. Vaidyanathan, "Coprime sampling and the MUSIC algorithm," in *Proc. IEEE Digital Signal Processing Workshop and IEEE Signal Processing Education Workshop*, Sedona, US, January 2011, pp. 289–294.

[11] F. S. Rawnaque and J. R. Buck, "Comparing the effect of aperture extension on the peak sidelobe level of sparse arrays," *Journal of the Acoustic Society of America Express Letters*, vol. 142(5), pp. 467–472, 2017.

[12] R. Schmidt, "Multiple emitter location and signal parameter estimation," *IEEE Transactions on Antennas and Propagation*, vol. 34, pp. 276–280, March 1986.

[13] C. L. Liu and P. P. Vaidyanathan, "Remarks on the spatial smoothing step in coarray MUSIC," *IEEE Signal Processing Letters*, vol. 22, no. 9, pp. 1438–1442, September 2015.

[14] K. Han and A. Nehorai, "Wideband gaussian source processing using a linear nested array," *IEEE Signal Processing Letters*, vol. 20, pp. 1110–1113, Nov 2013.

[15] K. Han and A. Nehorai, "Improved source number detection and direction estimation with nested arrays and ULAs using jackknifing," *IEEE Transactions on Signal Processing*, vol. 61, pp. 6118–6128, Nov 2013.

[16] S. Qin, Y. D. Zhang, and M. G. Amin, "Generalized coprime array configurations for direction-of-arrival estimation," *IEEE Transactions on Signal Processing*, vol. 63, no. 6, pp. 1377–1390, March 2015.

[17] Y. D. Zhang, M. G. Amin, and B. Himed, "Sparsity-based DOA estimation using co-prime arrays," in *Proc. IEEE ICASSP*, Vancouver, Canada, May 2013, pp. 3967 –3971.

[18] Q. Shen, W. Liu, W. Cui, and S. Wu, "Extension of co-prime arrays based on the fourth-order difference co-array concept," *IEEE Signal Processing Letters*, vol. 23, pp. 615–619, May 2016.

[19] M. I. Skolnik, *Introduction to Radar Systems*. New York, NY, USA: McGraw Hill, 2001.

[20] C. A. Balanis, *Antenna Theory: Analysis and Design*. New York, NY, USA: Wiley, 2016.

[21] B. Friedlander and A. J. Weiss, "Direction finding in the presence of mutual coupling," *IEEE Transactions on Antennas and Propagation*, vol. 39, no. 3, pp. 273–284, 1991.

[22] T. Svantesson, "Modeling and estimation of mutual coupling in a uniform linear array of dipoles," in *Proc. IEEE International Conference on Acoustics, Speech, and Signal Processing*, vol. 5, 1999, pp. 2961–2964.

[23] T. Svantesson, "Mutual coupling compensation using subspace fitting," in *Proc. IEEE Sensor Array Multichannel Signal Process. Workshop*, 2000, pp. 494–498.

[24] E. BouDaher, F. Ahmad, M. G. Amin, and A. Hoorfar, "DOA estimation with coprime arrays in the presence of mutual coupling," in *Proc. Eur. Signal Process. Conf.*, 2015, pp. 2830–2834.

[25] C. Liu and P. P. Vaidyanathan, "Super nested arrays: Linear sparse arrays with reduced mutual coupling Part I: Fundamentals," *IEEE Transactions on Signal Processing*, vol. 64, no. 15, pp. 3997–4012, August 2016.

[26] C. Liu and P. P. Vaidyanathan, "Super nested arrays linear sparse arrays with reduced mutual coupling Part II: Higher order extensions," *IEEE Transactions on Signal Processing*, vol. 64, no. 16, pp. 4203–4217, August 2016.

[27] J. Liu, Y. Zhang, S. Ren, and S. Cao, "Augmented nested arrays with enhanced DOF and reduced mutual coupling," *IEEE Transactions on Signal Processing*, vol. 65, pp. 5549–5563, 2017.

[28] R. Rajamki and V. Koivunen, "Sparse linear nested array for active sensing," in *2017 25th European Signal Processing Conference (EUSIPCO)*, Aug 2017, pp. 1976–1980.

[29] M. Yang, L. Sun, X. Yuan, and B. Chen, "A new nested MIMO array with increased degrees of freedom and hole-free difference coarray," *IEEE Signal Processing Letters*, vol. 25, no. 1, pp. 40–44, Jan 2018.

[30] J. Shi, G. Hu, X. Zhang, and H. Zhou, "Generalized nested array: Optimization for degrees of freedom and mutual coupling," *IEEE Communications Letters*, vol. 22, no. 6, pp. 1208–1211, June 2018.

[31] K. Adhikari and J. R. Buck, "Spatial spectral estimation with product processing of a pair of colinear arrays," *IEEE Transactions on Signal Processing*, vol. 65, pp. 2389–2401, May 2017.

[32] A. Raza, W. Liu, and Q. Shen, "Thinned coprime arrays for DOA estimation," in *Proc. of the European Signal Processing Conference*, 2017, pp. 395–399.

[33] Q. Shen, W. Liu, W. Cui, S. L. Wu, Y. D. Zhang, and M. Amin, "Low-complexity direction-of-arrival estimation based on wideband coprime arrays," *IEEE Transactions on Acoustics, Speech, and Language Processing*, vol. 23, pp. 1445–1456, Sep 2015.

[34] Q. Shen, W. Liu, W. Cui, and S. Wu, "Extension of nested arrays with the fourth-order difference co-array enhancement," in *2016 IEEE International Conference on Acoustics, Speech and Signal Processing (ICASSP)*, March 2016, pp. 2991–2995.

[35] D. A. Linebarger, I. H. Sudborough, and I. G. Tollis, "Difference bases and sparse sensor arrays," *IEEE Transactions on Information Theory*, vol. 39, no. 2, pp. 716–721, March 1993.

[36] Golomb Rulers and Costas Arrays. [Online]. Available: http://datagenetics.com/blog/february22013/